Supporting Information

Insights into Bulk Properties and Transport Mechanisms in New Ternary Halide Solid Electrolytes: First-Principles Calculations

Jiahao Qiu, Musheng Wu, * Wenwei Luo, Bo Xu, * Gang Liu, and Chuying Ouyang*

College of Physics, Communication and Electronics, Laboratory of Computational Materials Physics, Jiangxi Normal University, Nanchang 330022, China.

* **E-mail: smwu@jxnu.edu.cn; bxu4@mail.ustc.edu.cn; cyouyang@jxnu.edu.cn.**

Geometry structures

According to X-ray diffraction (XRD) Rietveld refinement results reported by Asano et al.,[1] the trigonal LYC with $p\bar{3}m1$ space group and the monoclinic LYB with $c2/m$ space group not only exhibit hcp and fcc anions sublattice, respectively, but also have a third of octahedral vacancy sites in the stoichiometric LYC and LYB, and resulting in Li partial occupancy of 6h/6g sites in LYC and 4h sites in LYB, respectively. To determine the Li configurations with lowest energies, we first generated 16 and 3 independent structures by enumerating possible site ordering of Li-ions in 6h/6g and 4h for LYC and LYB, respectively, as shown in Figure S1 and Figure S2. Then, all configurations were conducted DFT calculations to identify the geometries with the lowest energy, and the total energies of all configurations are also presented in Figure S1 and Figure S2.

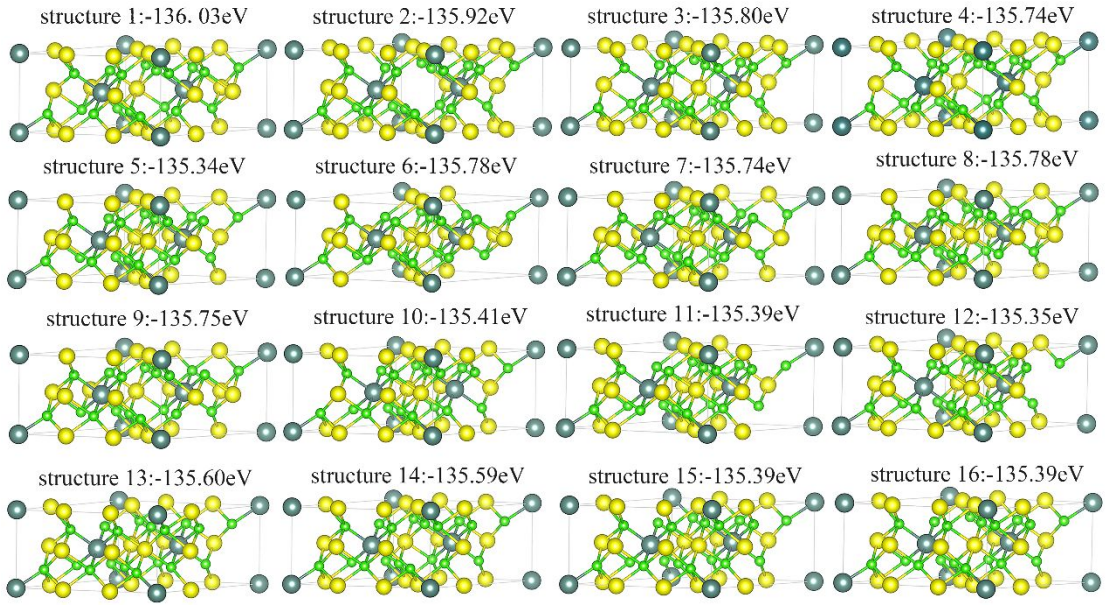

Figure S1 Ordering of Li-ions and corresponding total energies in LYC

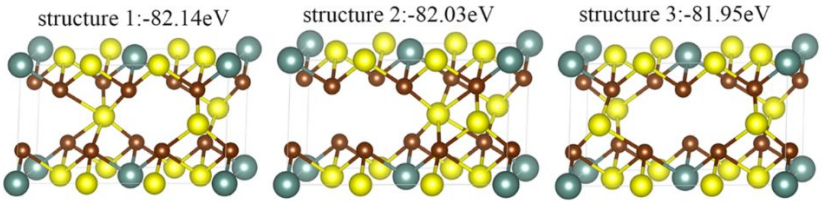

Figure S2 Ordering of Li-ions and corresponding total energies in LYB

Mechanical properties

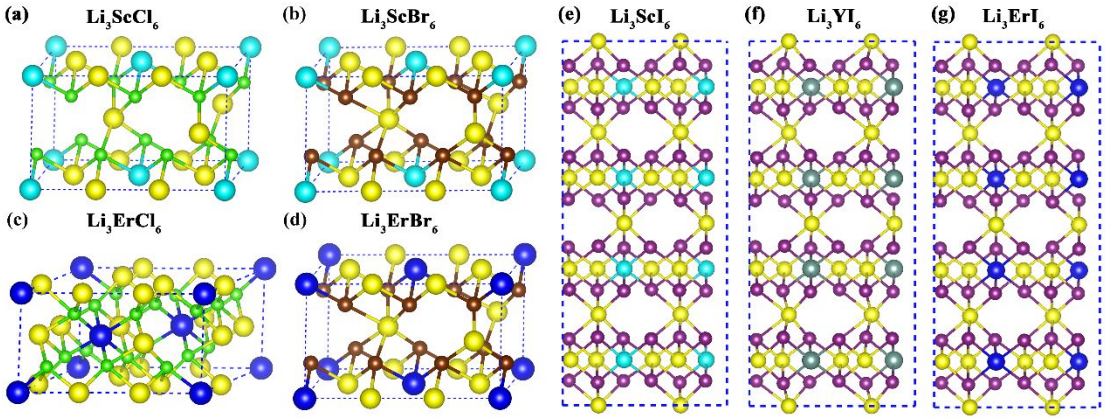

Figure S3 The crystal structures of (a) LScC, (b) LScB, (c) LErC, (d) LErB, (e) LScI, (f) LYI, and (g) LErI. The pale-blue, blue, cadet-blue, yellow, green, saddle-brown, and purple spheres represent Sc, Er, Y, Li, Cl, Br, and I atoms.

Table S1 the lattice parameters of all LMX except LYC and LYB

LMX	Space Group	a(Å)	b(Å)	c(Å)	α(°)	β(°)	γ(°)
Li_3ScCl_6	C2/m	6.446	11.004	6.464	90	109.21	90
Li_3ScBr_6	C2/m	6.810	11.780	6.889	90	107.54	90
Li_3ErCl_6	$P\bar{3}m1$	11.053	11.191	6.173	90	90	119.59
Li_3ErBr_6	C2/m	6.956	11.975	6.960	90	109.45	90
Li_3ScI_6	C2	7.429	12.954	29.099	90	90.34	90
Li_3YI_6	C2	7.556	13.154	29.003	90	90.25	90
Li_3ErI_6	C2	7.493	13.018	28.906	90	93.90	90

Table S2. The elastic constants (C) of all considered LMXs in this work, unit: GPa.

elastic constants	LYC	LErC	LScC	LYB	LScB	LErB	LScI	LYI	LErI
C_{11}	50.49	44.62	34.44	26.47	29.22	26.73	23.46	20.64	21.95
C_{12}	18.51	15.83	10.95	8.18	8.84	8.01	7.08	5.71	5.91
C_{13}	6.76	7.12	5.55	5.32	4.2	4.88	3.33	2.79	2.58
C_{14}	-2.52	-1.94	-	-	-	-	-	-	
C_{15}	-	-	1.02	1.12	-0.003	0.96	1.18	0.23	0.34
C_{22}	-	-	43.41	30.11	32.08	30.62	23.02	20.06	22.23
C_{23}	-	-	4.98	4.38	3.05	4.28	2.78	2.85	2.57
C_{25}	-	-	-3.04	-2.56	-3.05	-2.02	-0.69	-1.66	-1.67
C_{33}	40.76	30.9	26.5	23.81	19.94	22.45	16.29	15.11	15.02
C_{35}	-	-	-3.56	-2.7	-4.69	-2.12	-2.48	-1.83	-2.13
C_{44}	12.56	10.05	3.23	4.07	2.61	3.69	3.24	2.65	2.76
C_{46}	-	-	-2.47	-1.91	-2.36	-2.08	-0.89	-1.53	-1.63
C_{55}	-	-	6.1	7.04	3.45	5.6	1.56	2.26	2.05
C_{66}	-	-	15.12	11.3	11.69	11.02	8.19	7.43	8.1

Born stability criteria:

For trigonal crystals (LYC and LErC):[2]

$$C_{44} > 0,\ C_{11} > |C_{12}|, \quad (1)$$

$$(C_{11} + C_{12})C_{33} > 2C_{13}^2, \quad (2)$$

$$(C_{11} - C_{12})C_{44} > 2C_{14}^2, \quad (3)$$

For monoclinic crystals (the rest of LMXs) are given by:[3]

$$C_{ii} > 0 (i = 1\tilde{}6), \quad (4)$$

$$[C_{11} + C_{22} + C_{33} + 2C_{12}(C_{12} + C_{13} + C_{23})] > 0, \quad (5)$$

$$(C_{33}C_{55} - C_{35}^2) > 0, \quad (6)$$

$$(C_{44}C_{66} - C_{46}^2) > 0, \quad (7)$$

$$(C_{22} + C_{33} - 2C_{23}) > 0, \quad (8)$$

$$[C_{22}(C_{33}C_{55} - C_{35}^2) + 2C_{23}C_{25}C_{35} - C_{23}^2C_{55} - C_{25}^2C_{33}] > 0, \quad (9)$$

$$\{2[C_{15}C_{25}(C_{33}C_{12} - C_{13}C_{23}) + C_{15}C_{35}(C_{22}C_{13} - C_{12}C_{23}) + C_{25}C_{35}(C_{11}C_{23} - C_{12}C_{13})] - [C_{15}^2(C_{22}C_{33} - C_{23}^2) + C_{25}^2(C_{11}C_{33} - C_{13}^2) + C_{35}^2(C_{11}C_{22} - C_{12}^2)] + C_{55} g\} > 0 \ , \quad (10)$$

$$g = (C_{11}C_{22}C_{33} - C_{11}C_{23}^2 - C_{22}C_{13}^2 - C_{33}C_{12}^2 + 2C_{12}C_{13}C_{23}.$$

The bulk moduli and shear moduli can be obtained by the following expression:

$$B_V = \frac{1}{9}[(C_{11} + C_{22} + C_{33}) + 2(C_{12} + C_{23} + C_{31})], \quad (11)$$

$$G_V = \frac{1}{15}[(C_{11} + C_{22} + C_{33}) - (C_{12} + C_{23} + C_{31})] + \frac{1}{5}(C_{44} + C_{55} + C_{66}), \quad (12)$$

$$\frac{1}{B_R} = (S_{11} + S_{22} + S_{33}) + 2(S_{12} + S_{23} + S_{31}) \ , \quad (13)$$

$$\frac{1}{G_R} = \frac{4}{15}[(S_{11} + S_{22} + S_{33}) - (S_{12} + S_{23} + S_{31})] + \frac{1}{5}(S_{44} + S_{55} + S_{66}) \ , \quad (14)$$

$$B = \frac{B_V + B_R}{2}, \quad (15)$$

$$G = \frac{G_V + G_R}{2}. \quad (16)$$

Where B_V, B_R, B, and G_R, G_V, G are bulk moduli and shear moduli obtained from the Voigt (V), [4] Reuss (R), [5] and Hill schemes, respectively. S_{ij} are the elastic compliance constants, and are described by $S_{ij} = C_{ij}^{-1}$. For trigonal crystals, C_{11}=C_{22}, C_{13}=C_{23}=C_{31}, C_{44}=C_{55}, C_{66}=(C_{11}-C_{12})/2, and S_{11}=S_{22}, S_{13}=S_{23}=S_{31}, S_{44}=S_{55}, S_{66}=2(S_{11}-S_{12}). For monoclinic crystals, C_{13}=C_{31}, and S_{13}=S_{31}.

Li-ion diffusion mechanism

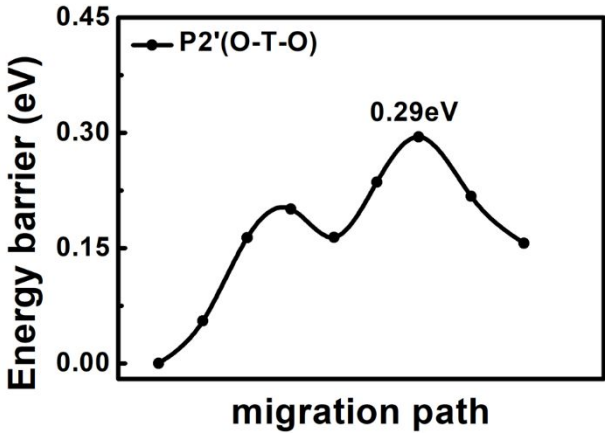

Figure S4 The migration energy barrier of Li-ion along P2′.

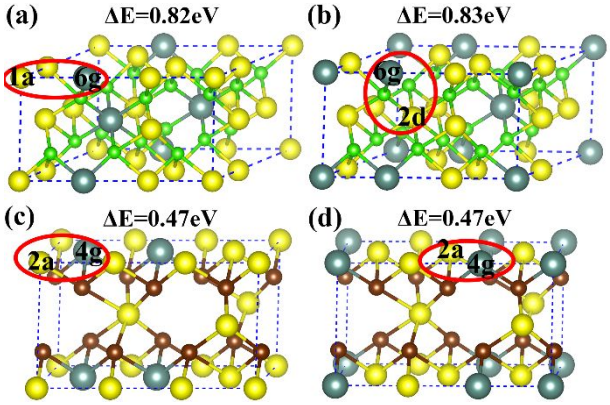

Figure S5. The representative disorder structures and energy differences of single Y and Li anti-site referencing to the lowest energy configure for (a)-(b) LYC and (c)-(d) LYB.

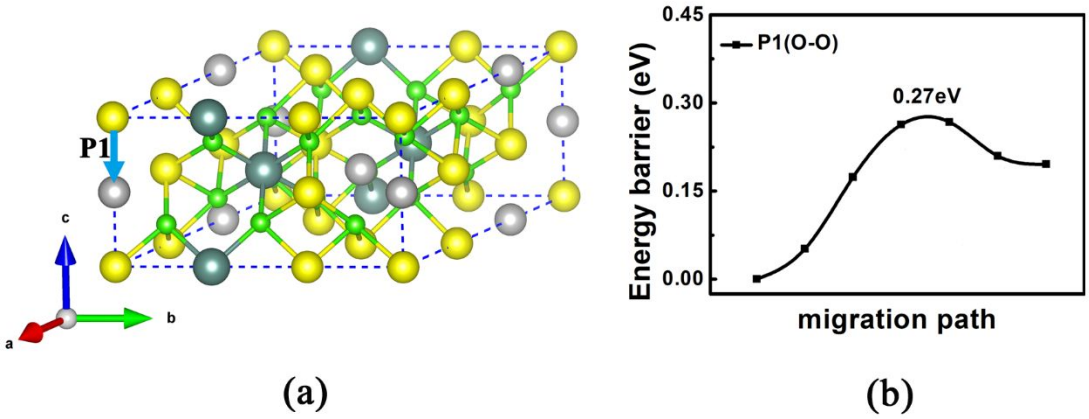

Figure S6. (a) The migration pathway along *c* direction, and (b) the corresponding energy barrier in single Y and Li anti-site configuration for LYC.

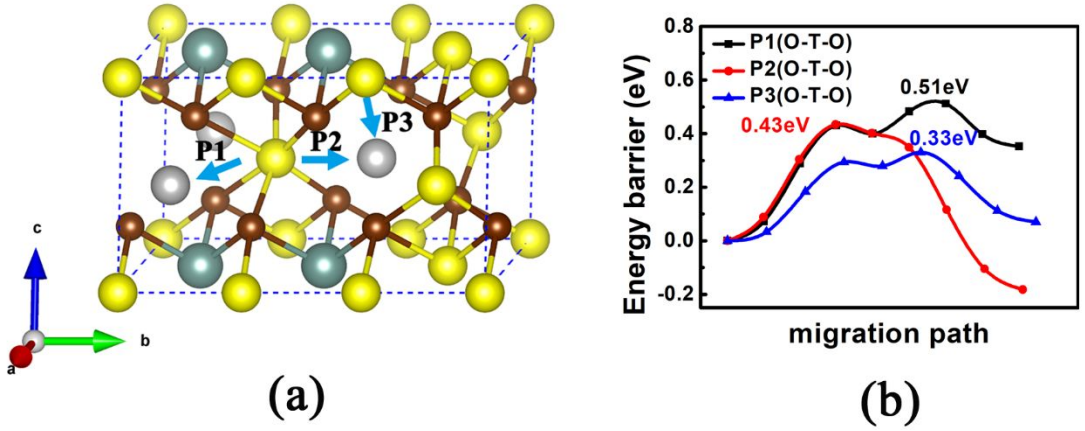

Figure S7. (a) The migration pathways and (b) the corresponding migration energy barrier of single Y and Li anti-site in LYB.

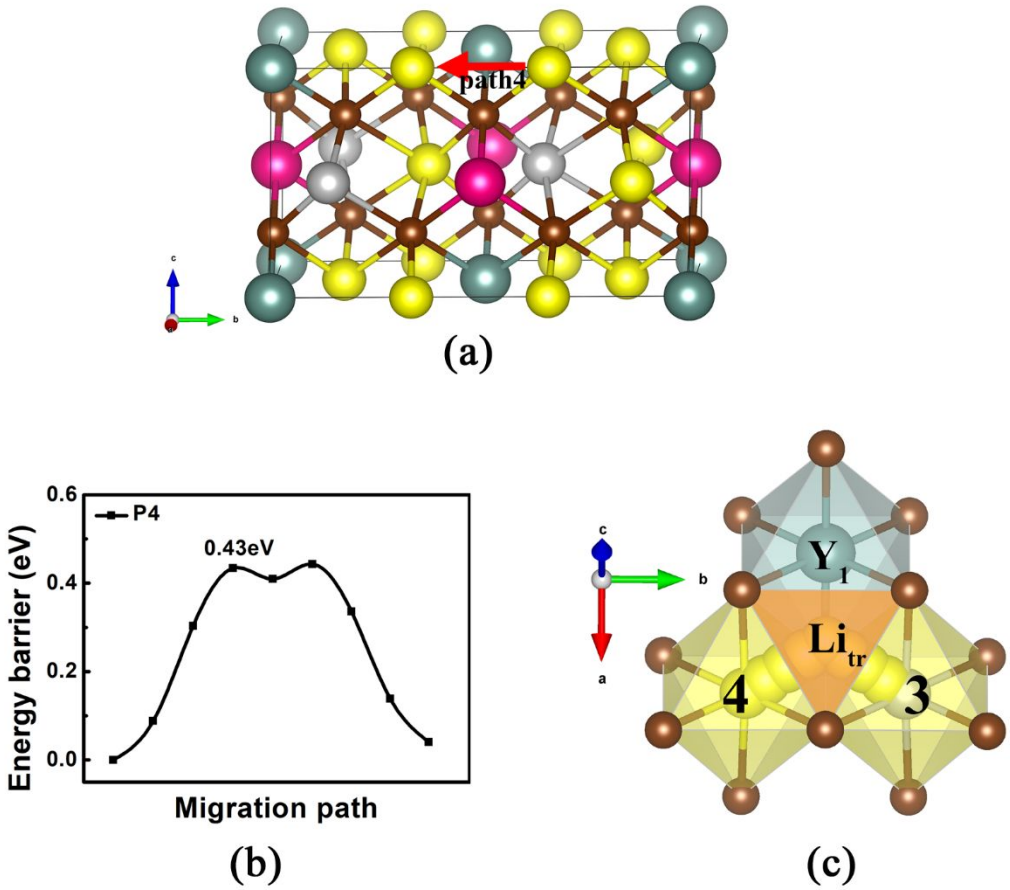

Figure S8 (a) Schematic drawing of single Li-ion migration along (001) plane, (b) energy profile of a Li-ion along P4, (c) the Li-ion local migration image along P4 pathway.

■ REFERENCES

(1) Asano, T.; Sakai, A.; Ouchi, S.; Sakaida, M.; Miyazaki, A.; Hasegawa, S. Solid Halide Electrolytes with High Lithium-Ion Conductivity for Application in 4 V Class Bulk-Type All-Solid-State Batteries. *Adv. Mater*. **2018**, *30*, 1803075.

(2) Mouhat, F.; Coudert, F.-X. Necessary and Sufficient Elastic Stability Conditions in Various Crystal Systems. *Phys. Rev. B*. **2014**, *90*, 224104.

(3) Wu, Z.-J.; Zhao, E.-J.; Xiang, H.-P.; Hao, X.-F.; Liu, X.-J.; Meng, J. Crystal structures and elastic properties of superhard IrN_2 and IrN_3 from first principles. *Phys. Rev. B*. **2007**, *76*, 054115.

(4) Voigt, W. Lehrburch der kristallphysik, Teubner, Leipzig. *New York: Macmillan.* **1928**, pp, 313-315.

(5) Reuss, A. Berechnung der fließgrenze von mischkristallen auf grund der plastizitätsbedingung für einkristalle. *ZAMM-J. Appl. Math. Mech*. **1929**, *9*, 49-58.